ERS Wind Scatterometer Commissioning and in-flight Calibration

NOAA / NESDIS Workshop
Operational use of Scatterometer Measurements of the Ocean Surface Wind Field

Pascal Lecomte
ERS Mission Coordination and Product Assurance Section, ESRIN, Frascati, Italy
Guy Brooker
Vega, Leiden, The Netherlands

On the 26th March 1996, the ERS-2 Scatterometer Commissioning Phase Working group declared that ERS-2 scatterometer data were ready for distribution to end-users.

This was the last step after nearly one year of work, firstly to find a way to recover the scatterometer, and secondly to perform in-flight characterisation of the instrument.

The scope of this paper is to present the objectives of the calibration and Validation activities, to detail the methods used to fulfil these objectives, and to present some early results.

1 Introduction

On the 21st April 1995, exactly one year ago, the second European Remote sensing Satellite, ERS-2 was launched from Kourou in French Guyana (see figure 1).

Six months prior to launch, a working group was setup in order to ensure proper calibration of the instrument and validation of the product distributed to the users.

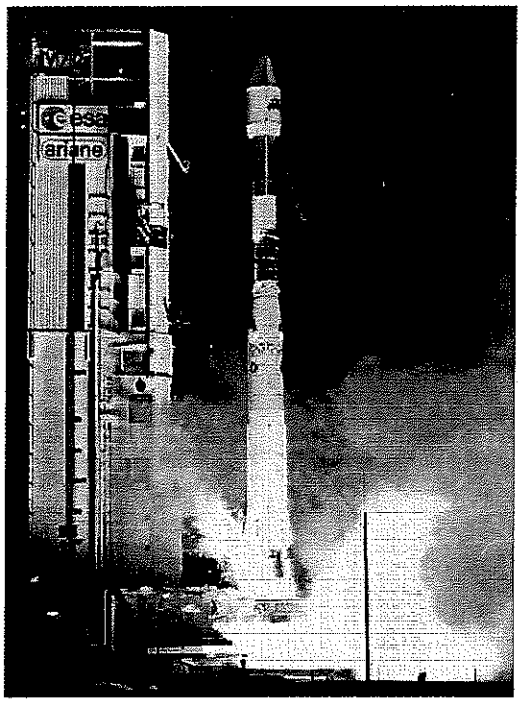

Figure 1: 21 April 1995: ERS-2 launch.

The strategy initially proposed for Engineering Calibration, and the results achieved are described herein.

Other papers, presented during this workshop, give a description of the instrument, the geophysical validation of the user products and the strategy used for routine quality control of the instrument.

ERS Scatterometer instrument

The Scatterometer on ERS satellites is combined with a Synthetic Aperture Radar (SAR) into the single Active Microwave Instrument (AMI).

The AMI operates in either SAR or Scatterometer mode. Nominally the instrument is in a combined wind/wave mode, making Scatterometer measurements interspersed with small SAR imagettes, which are used to derive wave spectra. These operations are interrupted for the acquisition of SAR Images, at the request of end-users.

First Scatterometer data

During the initial spacecraft testing, the first attempt to switch on the AMI resulted in a serious anomaly causing the instrument to shut down, both in SAR and Scatterometer modes. It was soon discovered that the instrument was prevented from working at nominal power. By reducing the output power to the minimum, engineers succeeded in acquiring the first SAR image on the same day, but it was still not possible to run the instrument in Wind mode.

Many tests were made to determine the cause and possible solutions to the problem. For more than six months the only data received from the

scatterometer was limited to few calibration pulses and echoes at each test, with no more than six echoes in a row before the instrument shut down.

On the 29th September 1995 more echoes were received than during all the months since launch, when the instrument was operated for an entire orbit.

The anomaly was resolved by setting the redundancy switch at the input to the High Power Amplifier to an intermediate position, thereby using it as a voltage spliter. The output power was reduced by a factor of two, and, for the first time some wind measurements could be made.

After the resolution of a few minor problems involving the system stability in the new configuration, the instrument went into the everyday satellite operations plan on the 2nd of November 1995.

2 Calibration and Validation objectives

At the engineering level, the result of processed scatterometer data are radar backscattering coefficients, σ^0, across the range of incidence angles of the instrument, for each of the three beams. These are then used to derive wind speed and direction using a wind to backscatter model (inversion).

The objectives of engineering calibration are to ensure that the σ^0 which is expected from a known target, is measured by the instrument (absolute calibration), and that the variation over the range of incidence angles of the instrument is unaffected by local attenuation from the antennae (relative calibration).

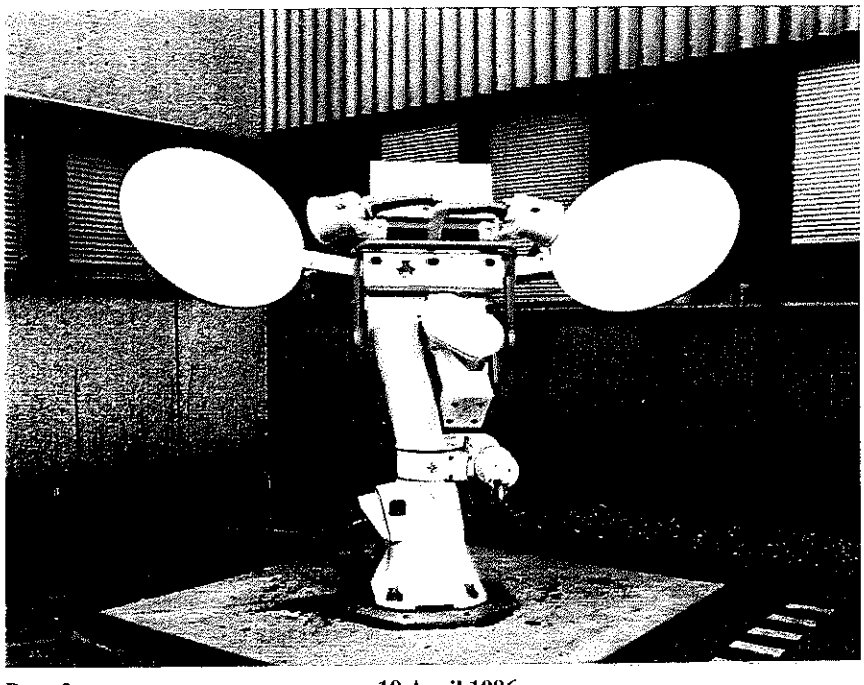

Figure 2: ERS Scatterometer Transponder during testing at Estec.

An absolute radiometric calibration of 0.7 dB is needed to satisfy the geophysical data quality requirements in terms of wind speed and direction.

This is achieved using a combination of internal and external references. Two different types of external references are used, point targets (transponders) and distributed targets (areas of known, constant backscatter).

Three transponders, one of them shown on figure 2 during testing at Estec, are installed in the South of Spain (figure 3). This position facilitates measurements at two or more incidence angles every three days. They are arranged in a line, spaced over hundreds of kilometres, such that all three may be illuminated by each scatterometer beam during an ascending or a descending pass. Additionally passes where two transponders are illuminated by one or more beams are used.

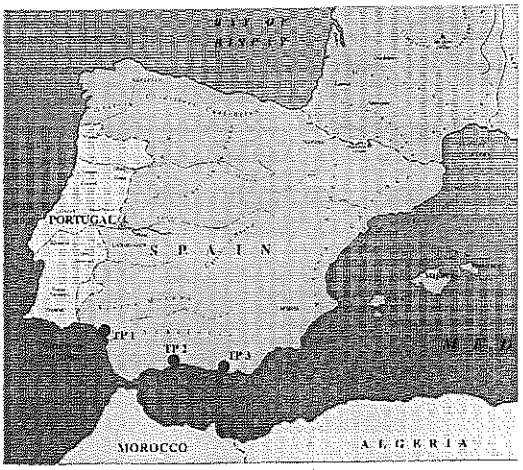

Figure 3: Scatterometer Transponder location South of Spain.

Each pass over a transponder allows the measurement error in backscatter at a particular incidence angle, to be computed from the power of the returned signal, and that measured at the transponder. The observation time of the transponders (in range and in azimuth) is used to verify proper antennae pointing.

After ERS-2 commissioning, two transponders will remain for monitoring purposes.

Although the transponders give accurate measurements of antenna attenuation at particular points within the antenna pattern, they are not adequate for fine tuning across all incidence angles, as there are simply not enough samples. This could be solved by deploying and operating a large number of transponders, so that many measurements can be made across the

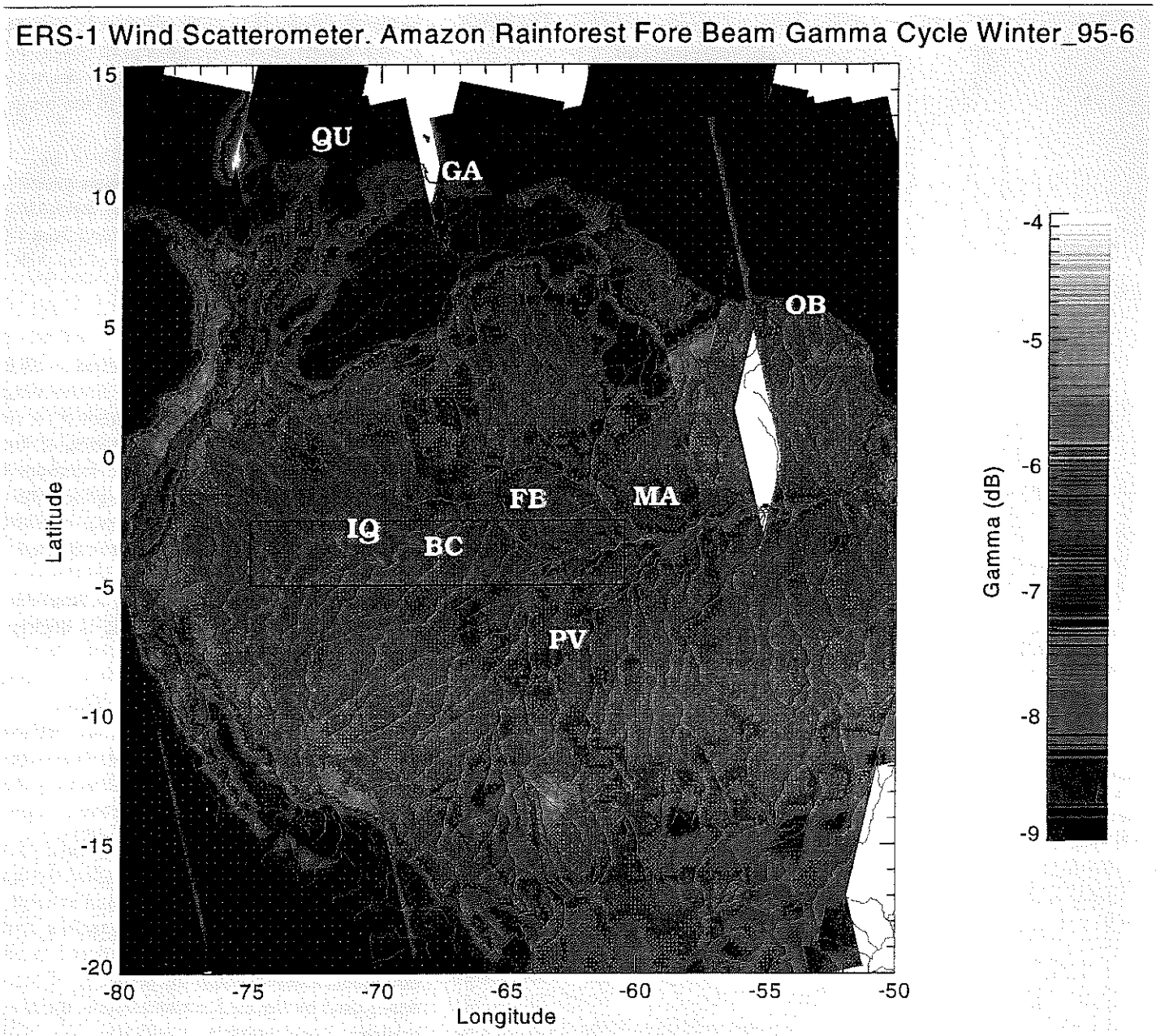

Figure 4: Amazonian Forest: Test area.

entire swath. Fortunately this enormous expense can be avoided by making use of large scale natural targets with a known response.

The tropical rain forest in South America has been used as a reference distributed target. The target is assumed to be isotropic and time invariant. Radar backscatter from the rain forest is shown on figure 4, as it was imaged by the ERS-2 scatterometer. This image shows the σ^0 of the rain forest corrected for the effect of illuminating the scene over a range incidence angles. This demonstrates clearly the uniform rain forest radar backscattering signature. Rivers, towns and mountains have a lower or higher σ^0 and consequently show up as dark or bright patches in the image.

The primary goal of the ERS-2 scatterometer calibration was to provide continuity to the users of ERS-1 scatterometer data. It was assumed that once the engineering calibration was complete, in terms of σ^0, that the wind derivation, and in particular the C-Band model used to compute the wind from the σ^0, was identical.

Prior to launch, the engineering parameters such as the antenna pattern or the on board gain, were set using the results of the on-ground characterisation of the instrument. Following launch, and the subsequent recovery of the instrument, the transmit power was lower, due to the initial anomaly.

The commissioning phase activities were then limited to the following activities:

- Set the on-board receiver gain

- Derive the antenna pattern correction for the three antennae from the rain forest and transponder measurements,
- Compute the antennae mispointing,
- Compute the calibration coefficients, and generate the associated Look Up Tables,
- Verify the stability of ERS-2 raw data (monitoring of the Long Term Stability of the instrument),
- Compare the ERS-1 and ERS-2 response over rains forest and transponders.

3 Receiver Gain Setting

ERS-1 on-board gains were optimised to ensure maximum use of the dynamic range of the analog to digital converter (ADC), whilst avoiding saturation. The initial ERS-2 on-board gains were set to the same level as for ERS-1.

The operational ERS-2 transmit power is approximately half the original setting, and also that of ERS-1. The configuration of the on-board receiver gain was not changed at the beginning of the commissioning phase. This allowed the stability of the instrument to be monitored for a number of months after operations began.

The ERS scatterometer processing is independent of the receiver gain setting, and small variations in on-board transmit power. This is acheived by scaling the incoming echoes by the ratio of the expected calibration pulse level, against the calibration pulse measured on board at the same moment. Thus changing the receiver gain, results in an increase or decrease in the echoes, and a similar effect in the measured calibration pulses.

Once the first corrections to the antenna patterns were made, and the stability of the instrument verified, the receiver gain was modified from 18 dB to 21 dB to take full advantage of the ADC dynamic range.

4 Antennae Mispointing

Two of the three scatterometer antennae on ERS are mechanically deployed. Small mispointing errors of the antennae may be corrected for in the ground processing. The orientation of the normal to each antenna plane can be determined using the transponders, by measuring the difference between the time the peak signal of each beam is observed, and when they are expected.

This analysis performed on ERS-2 scatterometer data shows that the mispointing is negligible.

5 Antenna patterns

The in-flight antenna patterns are characterised using a combination of single point measurements from the transponders, and measuring the response over a known, stable distributed target.

The ERS scatterometers work in C-Band (5.3 GHz) which is sensitive to the backscattering due to the trees (leaves and sticks). Therefore, the rain forest acts as a very rough surface, and the incoming signal is equally scattered in all directions. Consequently, for the angle of incidence used by the ERS scatterometers, the normalised backscattering coefficient σ^0 will depend only on the surface effectively seen by the instrument.

This surface S' is directly linked to the incidence angle by the relation

$$S' = S \cdot \cos\theta$$

Definition of γ^0

One can define the following formula

$$\gamma^0_{linear} = \frac{\sigma^0_{linear}}{\cos\theta}$$

Using this relation, the γ^0 backscattering coefficients over the rain forest are independent of incidence angle, allowing the measurements from each of the three beams to be compared.

Figure 5: Average γ^0 over rain forest, before and after engineering calibration

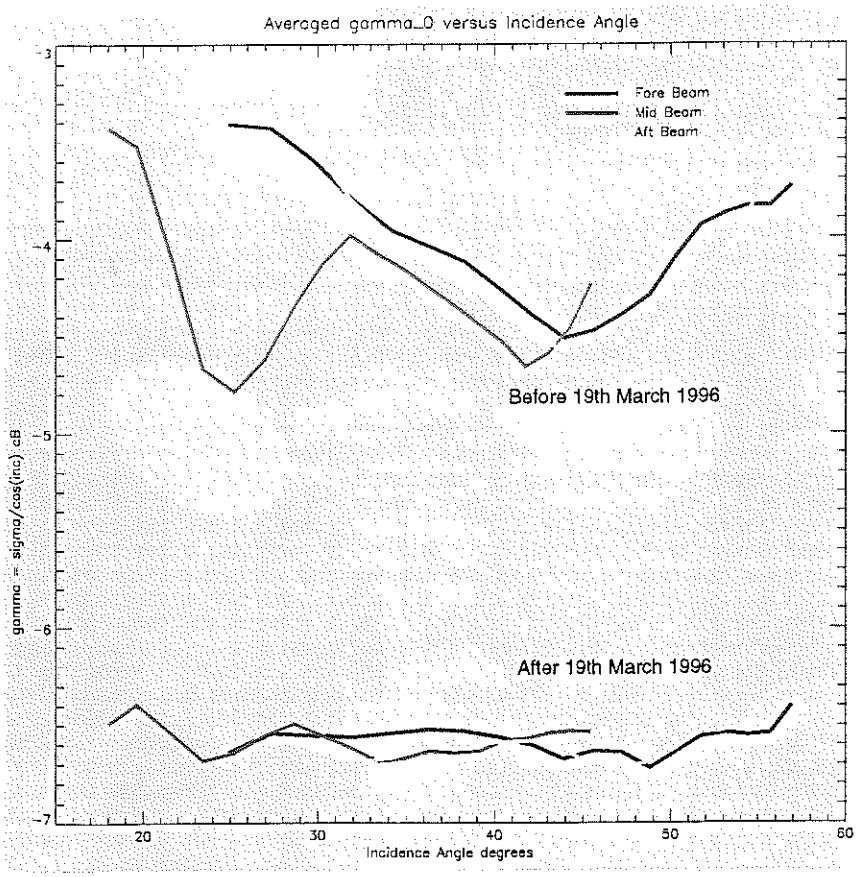

Thus if the assumptions of this relation are correct, then the γ^0 over such a target should be flat across the entire swath, and equal in all beams.

An area was chosen, shown in figure 4, which exhibits:

- Flat topography. (The incidence angle θ is computed with respect to the ellipsoid GM6, and not with respect to the real topography).
- No large scale deforestation.
- No large rivers, lakes or towns.
- Stable climate. (Rain and humidity influence the backscattered signal).

This test area is located between 2.5°S and 5.0°S in latitude and 60.5°W and 75.0°W in longitude.This area is not touched by deforestation and has limited urbanisation, lies south of the Amazon, and north east of the main mountain ranges of South America. Furthermore, this area has a low rain variation over the year. In fact, the comparison of the annual rain fall over the stations of Fonte Boa, Iquitos and Benjamin Constant ("FB", "IQ" and "BC" in figure 4) and other stations, show that the annual variation is lower over the test area. Still, this variation is not negligible as the annual variation is higher than 200 mm at Benjamin Constant. At this station, the annual minimum is during the period June to September.

Analysis of γ^0

The figure 5 shows a comparison of the γ^0 with respect to the incidence angle θ for the three beams of the ERS-2 scatterometer, before and after the instrument calibration.

The two side antennae (fore and aft) have nearly identical patterns. The deviation between the two curves are less than 0.3 dB. A more careful analysis of this data shows that the oscillation observed in these two curves can also be seen in the mid beam at an incidence angles 10° less. Thus it can be surmised that these anomalies correspond to the target and are probably due to small heterogeneity of the test area.

The second and the third nodes of the mid beam, which correspond respectively to an incidence angle of 19.6° and 21.7°, show a different effect. These two measurements give a value of γ^0 higher than that measured by the two other beams.

The deviation, +0.2 dB, is systematic and does not depend either on the period of the year, nor on the test area chosen. This may point to an anomaly in the characterisation of the mid antenna pattern.

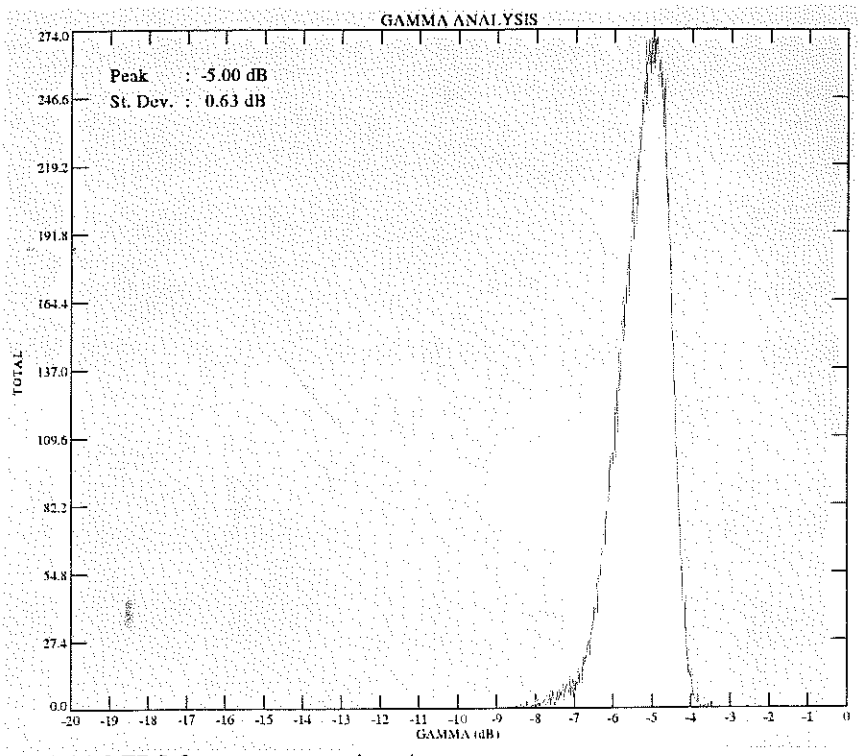

Figure 6: ERS-2 γ^0 distribution for beginning of April 1996

The initial ERS-2 pattern corrections have produced satisfactory results, and a fine tuning is under way.

6 Instrument stability

The instrument calibration pulses are used to measure the stability of the transmit/receive chain on-board. As mentioned above, the scatterometer processing automatically corrects for any variation measured by the calibration pulses. Changes in the antenna patterns over time may also occur, in the long term due to antenna degradation, and in the short term due to temperature variation around the orbit, and throughout the year.

As γ^0 is independent of incidence angle, a histogram of γ^0 over the rain forest is characterised by a sharp peak. Monitoring the position of the peak over time is one method to check the stability of the calibration.

Histograms are produced, one for each antenna ("Fore", "Mid" and "Aft") and one combining all the measurements ("Fore/Mid/Aft"). The histogram bin size is 0.02 dB. The mean and the standard deviation are computed directly from each distribution. The peak position is computed by fitting the histogram with a normal distribution added to a second order polynomial.

$$F\langle x\rangle = A_0 \cdot \exp\left(-\frac{z^2}{2}\right) + A_3 + A_4 \cdot x + A_5 \cdot x^2$$

$$with \qquad z = \frac{x - A_1}{A_2}$$

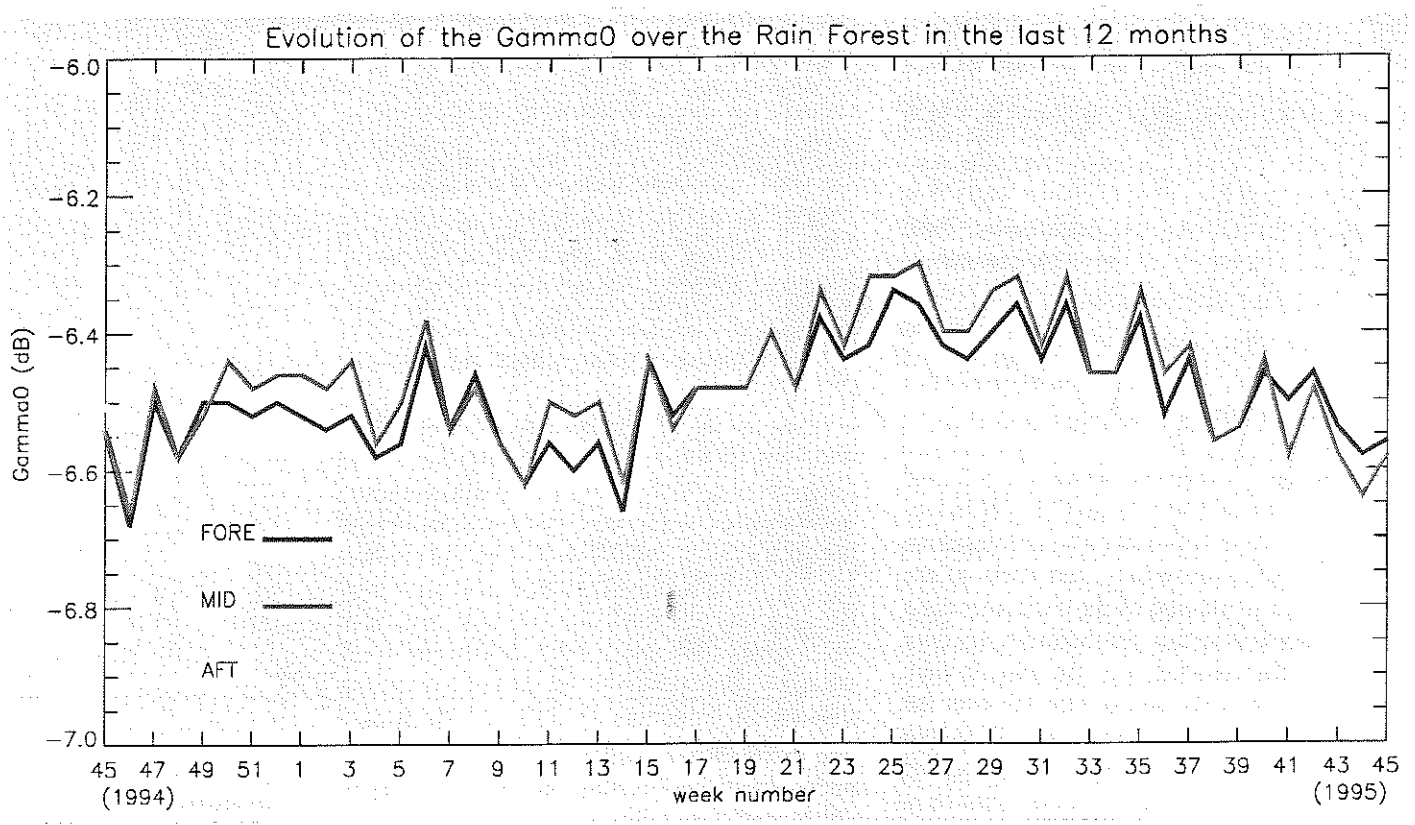

Figure 7: ERS-1 γ^0 distribution peak position time-series.

In this formulation, the normal distribution has a mean equal to A_1 and a standard deviation equal to A_2. The parameters A_0 to A_5 are computed by using a non linear least square method called "gradient expansion" [Bevington, 1969].

The position of the peak is given by the maximum of the function F.

This method gives much more precise results than a simple filtering method.

The histograms (figure 6) computed for ERS-2 with one of the first set of calibrated data acquired at the beginning of April 1996 over the test area show the following points:

- Unique peak,
- The peak positions for all beams are nearly identical
- The widths of the distributions are small (the standard deviations are lower than 0,35 dB)

The following table summarises the results for the end of March 1996.

γ^0	Mean	Peak position	Standard deviation
Fore	-6.48 dB	-6.44 dB	0.29 dB
Aft	-6.46 dB	-6.44 dB	0.28 dB
Mid	-6.61 dB	-6.56 dB	0.32 dB
All	-6.51 dB	-6.48 dB	0.30 dB

This demonstrates that the assumptions of the γ^0 have some foundation, and that γ^0 is useful as a comparison of the measurements made with the three antenna without having to take into account the incidence angles.

The following conclusions can be drawn:

- There is a slight deviation between the peak position and the mean of the distribution; i.e. that the distributions are not symmetrical.
- The standard deviation of the Mid beam is higher than the for the two other antennae. This can be due to two reason: first the noise on the mid beam is slightly higher. Secondly the higher γ^0 measured on the mid beam at low incidence angles (node two and three) is not corrected for when constructing the histograms and introduces noise in the γ^0 distribution.
- Taking in to account the noise observed in the measurements, the peak position for the Fore and Aft antennae are equal; the mid beam has a slightly higher signal (+0.1 dB).

ERS-1 Annual stability

The Long term stability of the scatterometer is an important element of the Calibration activities. It has to be seen as the extension of the commissioning phase across the all life time of the instrument.

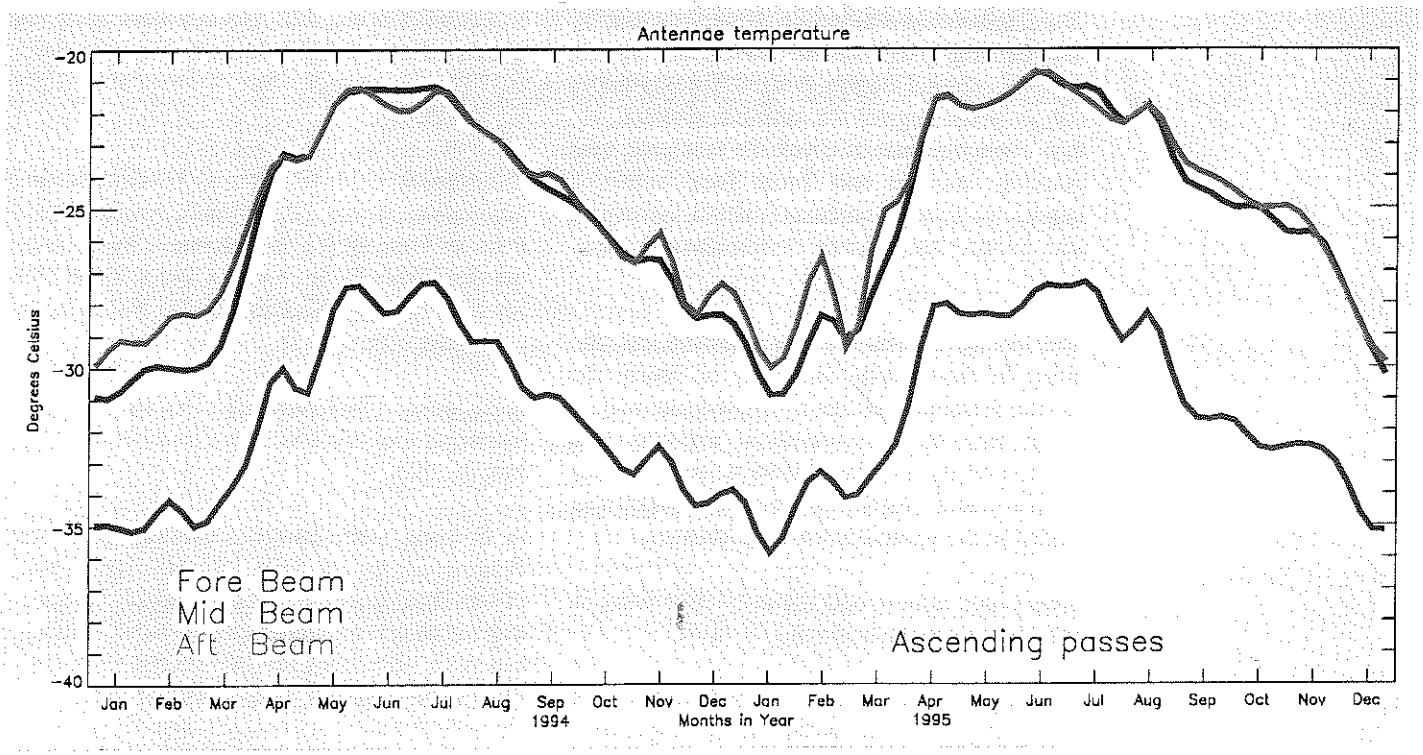

Figure 8: ERS-1 Antennae temperature over the test site for ascending passes

For the ERS missions, the peak position of the γ^0 distribution is weekly monitored in parallel to the transponders activities.

The figure 7 shows the ERS-1 peak position time series for the three antennae over the period November 1992 to November 1993.

The analysis of these curves demonstrate the stability over the whole period, even if a small oscillation can be detected. It is also noteworthy that the three antennae have very similar γ^0 evolution (around -6.5 dB).

The mid beam gives an higher signal most of the time; this deviation is approximately 0.1 dB from the Fore beam in May and July 1992. The fore and aft beams have very similar responses. One can see a seasonal variation in all three antennae. This signal has an amplitude of 0.2 dB.

Comparisons of the γ^0 time-series with the rain fall measurements at Benjamin Constant show that the data do not correspond. The maximum γ^0 is seperated by three months from the minimum rainfall.

Antennae Temperature

The most probable effect on γ^0 stability is the variation of antennae temperature over the test site along the year (figure 8 on page 7).

The antennae temperature along the orbit varies with the illumination from the sun. It appears that the temperature change is rather slow increasing continuously during satellite illumination and decreasing continuously in shadow.

The test area used to measure the stability of the instrument is close to the equator and limited in size. During the descending passes (i.e. during sun illumination), the temperature of the antennae over the test area will depend on the period of time the satellite was illuminated by the sun.

This varies with the season and is maximum at the summer solstice and is minimum during winter. The maximum of temperature over the test area for the ascending passes is during winter and the minimum during summer. Along the year, the overall temperature over the site can vary by more than seven degrees.

Both during the ERS-1 and ERS-2 commissioning phases, the short term temperature stability were checked and proved to be well within specification. Although the ground processing can accomodate corrections for antennae temperature σ^0 variation, this functionality has not been used.

The long term monitoring shows that this temperature effect over the test site is minimal (0.15 dB), and demonstrates that this has a negligible effect on wind speed and direction.

7 Conclusion

Instrument commissioning and in-flight calibration is a major activity which required carefull preparation before launch.

The Engineering Calibration strategy chosen by the working group, relied extensively on two types of external targets, dedicated transponders (single point targets) for absolute antenna pattern correction and to check the antennae mispointing, and the rain forest (large isotropic target) for relative antennae pattern correction and Sensor Long Loop Performance Assessment.

This strategy proved to be very flexible and efficient. In fact despite the delay of nearly six months introduced by the instrument anomaly, a major step in the calibration activities was reached on the 19 March 1996 when a new set of instrument characterisation parameters was loaded in the ground processing facilities.

ERS-2 data is now operationally distributed to end users since the beginning of April.

An additional fine tuning of the instrument is expected to complete the commissioning activities in May 1996.

ERS-2 data is still carefully checked every day in order to detect any anomaly in the frame work of the Operational monitoring of the instrument, but is now ready to take over from the ERS-1 scatterometer which shall be switch off and put on standby on the 2nd June 1996.

8 Bibliography

V. Amans, *ERS Wind Scatterometer Quality Control,* NOAA / NESDIS Woorkshop Proceedings, April 1996, Alexandria, VA, USA.

E. Attema, *Estimating Satellite Pointing biases from Scatterometer transponder Measurements - An exact Solution,* ORM/3078/EA/sml, 14 March 1989.

E. Attema, *The Design, Calibration and System Performances of the ERS-1 and ERS- 2 Wind Scatterometer,* NOAA / NESDIS Woorkshop Proceedings, April 1996, Alexandria, VA, USA.

A. Cavanié, P. Lecomte, *Study of a method to dealiase winds from ERS-1 data,* ESA contract 6874/87/GP-I(sc), 1987.

R. Graham et al., *Evaluation of ERS-1 Wind Extraction and Ambiguity Removal Algorithms,* ESA Contract. January 1989.

D. Guyenne ed., *ERS-1 A new tool for global environmental monitoring in the 1990's,* ESA BR-36, November 1989, ESTEC, Noordwijk. The Netherlands, (ISBN 92-9092-019-X).

P. Lecomte et al., *ERS product Assurance and Quality Control,* ESA Bulletin 82, May 1995, ESTEC, Noordwijk. The Netherlands, (ISSN 0376-4265).

P. Lecomte, E. P. W. Attema, *Calibration and Validation of the ERS-1 Wind Scatterometer,* Proc. of First ERS-1 Symposium - Space at the Service of our Environment, Cannes 1992, ESA SP-359, ESTEC, Noordwijk, The Netherlands, (ISBN 92-9092-278-8).

P. Lecomte, *CMOD4 Model Description,* ESA technical note ER-TN-ESA-GP-1120, Rev. 1.2, March 1993.

A. E. Long 1985, *Toward a C-Band Radar Sea Echo model for the ERS-1 Scatterometer,* Proc. of the Third International Colloquium on Spectral Signature of Objects in Remote Sensing, Les Arcs 1985, ESA SP-247, ESTEC, Noordwijk. The Netherlands, (ISSN 079-6566).

A. E. Long, *ERS-1 C-Band and Sea-Echo Models,* ESA internal Report ESTEC/WMA/9104, Rev. 1. April 1991.

N. Longdon ed., *ERS-1 Data Book,* ESA BR-75, April 1991, ESTEC, Noordwijk. The Netherlands, (ISSN 0250-1589).

O. Mestre, *Réponse du diffusiomètre d'ERS-1 en fonction de l'angle d'incidence,* note de travail de l'ENM 462.

D. Offiler, *Validation of ERS-1 Scatterometer winds; An Appraisal of Operational Backscatter Model Performances from launch to Present,* NOAA / NESDIS Woorkshop Proceedings, April 1996, Alexandria, VA, USA.

A. Stoffelen, D. Anderson, *Characterisation of ERS-1 scatterometer measurements and wind retrieval,* Proc. of Second ERS-1 Symposium - Space at the Service of our Environment, Hamburg 1993, ESA SP-361, ESTEC, Noordwijk, The Netherlands, (ISBN 92-9092-286-9).

P. Vass, B. Battrick ed., *ERS-1 System,* ESA SP-1146, September 1992, ESTEC, Noordwijk. The Netherlands, (ISSN 0379-6566).

M. Wooding ed., *ERS-1 Geophysical Validation,* Woorkshop Proceedings, ESA WPP-36, August 1992, ESTEC, Noordwijk, The Netherlands.